Malaysian Journal of Civil Engineering 27(3):437-449 (2015)

EFFECTS OF DISTANCE BETWEEN TWO T-SHAPED SPUR DIKES ON FLOW PATTERN IN A 90 DEGREE BEND USING NUMERICAL MODEL

Vaghefi Mohammad*, Safarpoor Yaser & Hashemi Seyed Shaker

Civil Engineering Department, Persian Gulf University, Shahid mahini street, Bushehr, Iran

*Corresponding Author: *Vaghefi@pgu.ac.ir*

Abstract: Spur dike is a type of flow control structure. Certain changes occur in flow pattern due to installation of a dike (especially a T-shaped spur dike). This paper studied the effects of distance between two T-shaped spur dikes on flow pattern in a 90° bend. The first spur dike was installed in the middle of bend at the outer bank and the second one was installed separately at distances of 2.5, 3.5 and 5 times the spur dike length. For each distance between the dikes, a numerical analysis was performed. It was observed that near the bed, the flow moved toward inner bank but on the water surface it moved toward outer bank. By increasing the distance between the dikes, the dimensions of vortexes increased. Near the bed and on the water surface, three vortexes were formed: (1) at upstream of the first dike,(2) in the dikes field and (3) at downstream of the second dike. The dimensions, numbers and location of vortexes changed by changing the distance between spur dikes. At upstream of the second dike, three vortexes were formed: (1) a central vortex, (2) a vortex near the bed in front of the dike wing and (3) a vortex at outer bank.

Keywords: *SSIIM Model, T-shaped spur dike, flow pattern, bend, vortex*.

1.0 Introduction

Spur dikes are usually used to protect river banks from erosion and keep the main channel navigable. Some of them are usually built in series. Many researches have been done on the studying of spur dikes. Shukry (1950) conducted the preliminary studies in the channel bend and presented an equation for calculating the power of secondary flow. Spacing-to-length ratios of spur dikes equal to 3 may be effective in protecting concave banks; however, some type of minimal protection may be needed along the banks. Spur dike roots should be protected from scour caused by vortices set up along the upstream and downstream faces (Copeland, 1983). In computing a turbulent flow, it is useful to decompose the instantaneous motion into mean and fluctuation velocity (Muto *et al*., 2002). Various types of groynes can be distinguished according to their construction, action on stream and appearance. The spacing between groynes is measured at the riverbank between their starting points. It is related to river width, groyne length, velocity of flow, bank curvature, and purpose.

For bank protection distances from 2 to 6 times of groyne length are generally used. If the spacing between groynes is too long, a meander loop may form between groynes (Yossef, 2002). Suzuki *et al*. (1987) conducted experiments on characteristics the movable bed around a series of spur dikes and found that the bed form around the spur dike has a significant impact on the relative distance between spur dikes. A spur dike may be submerged during the flood conditions, Elawady *et al*. (2001) studied the movable bed scour around submerged spur-dikes and showed that local scour around submerged spur dikes is significantly affected by the overtopping ratio and the opening ratio. Sukhodolov *et al*. (2004) have categorized the vortex patterns between the spur dikes based on the spur dike spacing. At a very small spacing, two small vortices with a transverse orientation occur inside the spur dike field. One of these vortices disappears as increase the spacing between the spur dikes. With a larger spacing between the spur dikes, two vortices develop with a longitudinal orientation inside the spur dike field.

Muto *et al*. (2002) with experimentally studies on flow velocity around spur dikes studied the flow patterns within the space enclosed between the spur dikes also the role of this space for creation of rotational currents investigated. Wildhagen (2004) showed that the SSIIM model is capable to simulate the flow and scour patterns in a sharply curved meandering channel. Naji Abhari *et al*. (2010) studied the numerical simulation in a 90° bend using SSIIM model (SSIIM is abbreviation for Sediment Simulation In Intakes with Multi block option); distributions of shear stress at the channel bed showed a tense region near the inner wall which moved to the outer bank at the end of the bend. One of the spur dikes that have a unique impact on the flow pattern (due to having a wing part) is T-shaped spur dike. The studies on this type of spur dike are limit. Ghodsian and Vaghefi (2010) by experimental study on scour and flow field in a scour hole around a T-shaped spur dike in a 90 degree bend showed that by increasing the wing length of spur dike, the zone of flow separation expands and the sizes of vortex increase.

Mousavi *et al*. (2010) investigated the effects of the bend relative radius on changing of vorticity value around a T-shaped spur dike; the maximum vorticity value occurred for relative curvature of 4 that present an interaction between spiral velocity value, scouring and relative radius. Mousavi *et al*. (2012) checked out the 3-dimensional numerical model and laboratory for flow and the bed deformation around a T-shaped spur dike in a 90° bend and showed that by increasing the ratio of curvature radius to width of bend, the strength of secondary flow decreases and the magnitude of velocity near the outer bank is increased, but the angle of collision of streamlines to the outer bank is decreased. Mansoori *et al*. (2012) studied the characteristics of the flow around spur dikes installed in a fluvial channel; the comparison between the T-shaped spur dikes and straight spur dikes showed that by installing T-shaped spur dikes in stream, distribution of high stress and high energetic zones around spur dikes as well as the main stream is more homogenous. Vaghefi *et al*. (2014) studied the effect of T-shaped spur dike submergence ratio on water surface profile in 90 degree bend using SSIIM model and concluded that at the water surface, flow moves toward the outer bank and the height of flow at outer bank is more than inner one. The lowest water level occurs in downstream near the inner bank. They also studied the effect of ratio on various submersions on three-dimensional velocity and concluded that with an increase in submersion of the spur dike, the flow changes into up flow behind the wing. Vaghefi *et al*. (2015) check out the effects of relative curvature on the scour pattern in a 90° bend with a T-shaped spur dike using SSIIM model; they were calibrated the SSIIM model for using in bend and studied the scoring pattern due to changes in flow pattern. Finally given the importance of the impact of the distance between spur dikes on the formation of various vortexes, two T-shaped spur dikes were analyzed in different situations. The flow patterns were compared together due to the dike locations under the influence of flow velocity and secondary flow. The main objective of this paper is identification of the effects of the distance between two spur dikes on the formation of vortexes and on the changes of the flow pattern. To achieve this, the flow patterns are shown at cross sections and at plans and are compared with each other. With the knowledge of flow patterns, the scour pattern of the channel bed will be determined. The scour pattern is an important point in the river organizing projects.

2.0 Materials and Methods

2.1 Numerical Model

The SSIIM numerical model solves the Navier-Stokes equations with the k-ε model on a 3-dimensional almost general non-orthogonal grid. The Navier-Stokes equations for turbulent flow in a general 3-dimensional geometry are solved to obtain the water velocity. The Navier-Stokes equations for non-compressible and constant density flow can be modeled as Equation (1).

$$\frac{\partial U_i}{\partial t} + U_j \frac{\partial U_i}{\partial x_i} = \frac{1}{\rho} \frac{\partial}{\partial x_i} \left(-P\delta_{ij} - \rho \overline{u_i u_j} \right) \tag{1}$$

Where x_1, x_2 and x_3 are distances and U_1, U_2 and U_3 are velocities in three directions. P is pressure, δ_{ji} is Kronecker Delta that is equal to unity for $i = j$ and is zero otherwise. The left term on the left side of the equation is the transient term. The next term is the convective term. The first term on the right-hand side is the pressure term. The second term on the right side of equation is the Reynolds stress term; to evaluate this term k-ε turbulence model was used. The SIMPLE method computes the pressure term (Olsen, 1999-2001 and Wildhagen, 2004). The sample of channel modeling has been shown in

Figure 1. (That S is distance between spur dikes, L is the spur dike length and Θ is the angle from the bend entry). In SSIIM-1 (Version 1) a structured grid is used. The grid systems in the vertical, lateral and longitudinal directions have respectively 26, 36 and 65 lines and in total have 60840 cells. The grid system is checked using a finer mesh, when the number of gridlines was doubled in all directions the computation time was very long which is not suitable for practical engineering purposes. Furthermore the results showed on affect on the accuracy of the solution by a refinement of the grid. The bed and wall roughness is chosen as a constant Strickler value kst=64 $m^{1/3}/s$. The effective roughness is computed as Van Rijn equation (Van Rijn, 2007).

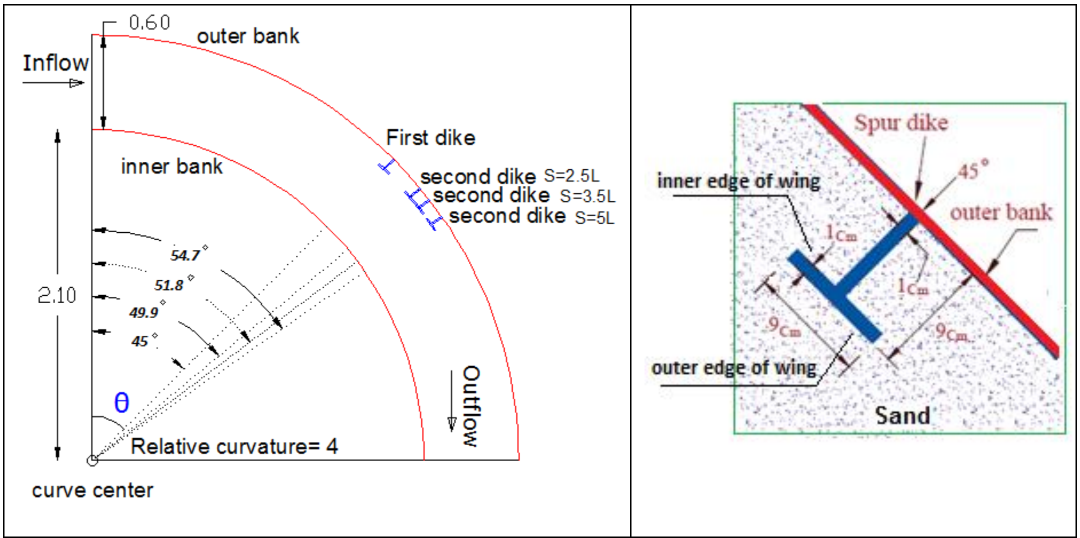

(a) Second dike was installed separately (b)

Figure 1: Channel plan (a) spur dikes location (b) details of spur dike

2.2 *Boundary Conditions*

The amount of discharge should be introduced in the entry and end of bend. The gradient of all parameters in the outputs boundary are zero. The flux passing the bed and walls is zero. As Equation (2), the wall law of Schlichting (1979) is used for wall friction of the bend in all cases. On water surface the zero gradient boundary conditions are used for the loss of turbulent kinetic energy. The turbulent kinetic energy is set to zero. Symmetrical boundary conditions are used for the water velocity, meaning zero gradient boundary conditions are used for the velocities in the horizontal directions. The velocity in the vertical direction is calculated from the criteria of zero water flux across the water surface.

$$\frac{U}{U^*} = \frac{1}{k} Ln\left({}^{30y}\!/_{k_s} \right) \tag{2}$$

Where U is velocity, U^* is shear velocity, k is a constant coefficient equal to 0.4, y is distance from wall to the center of the cell, that k_s is the roughness at wall (Olsen, 2000 and 2009).

2.3 Verification

The experiments was carried out in Hydraulics Laboratory of Tarbiat Modares University in Iran, on a laboratory flume with the width of 60 cm and the height of 70cm in a compound of straight and bend route. The length of straight upstream route is 710cm, and is connected to straight downstream route of 520cm via a 90° bend with an external radius of 270cm and an internal radius of 210cm. The spur dike used in this experiment is a T-shaped spur dike. The length of dike wing and web are equal to 9cm, with the height of 25cm. This spur dike is vertical and non-submerged in a 45° position. The ratio of bend radius to width of channel is equal to 4. The uniform sediments have an average diameter of 1.28mm. Also the flow discharge equals to 25 (liter/second). The standard deviation of bed particles is equal to 1.3, analysis is performed in clear water conditions.

The initial water depth in upstream of channel and in the start of bend is equal to 11.6cm. The Froude number of the flow in the bend entry is equal to 0.34, the walls of channel are rigid. Experiments time is 24 hours. The density of sediment particles equals to 2.35gram/cm^3 (Vaghefi *et al*. 2012). The time of solution is 24 hours for each experiment. At this time, the scour rate is less than 2 mm at 4-hour intervals. Comparisons the velocities at different sections (longitudinal sections and cross-sections) are shown as Figures 2-3. It is observed that the model is capable of providing flow pattern and is consistent with laboratory model and the SSIIM model could accurately simulate the flow pattern and 3-dimentional velocities in 90° bend and is applicable in this study.

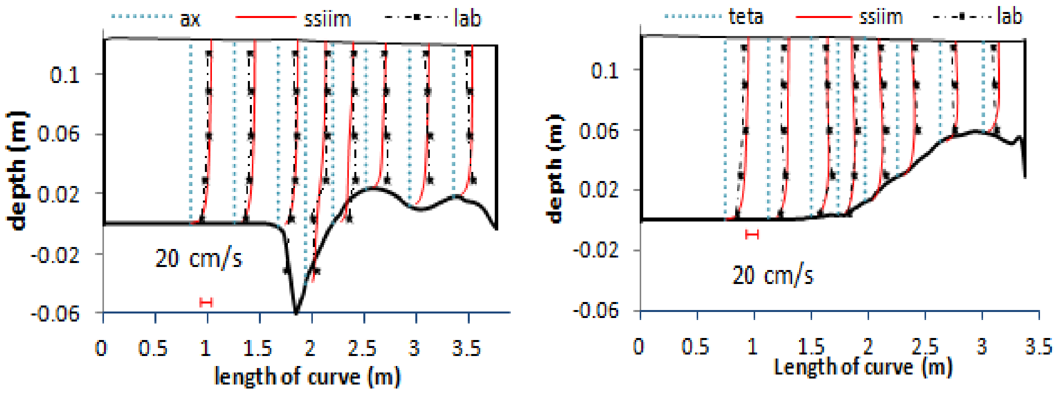

(a) (b)

Figure 2: Longitudinal velocity in longitudinal-section at a distance (a) 50% (b) 92% of channel width from outer bank

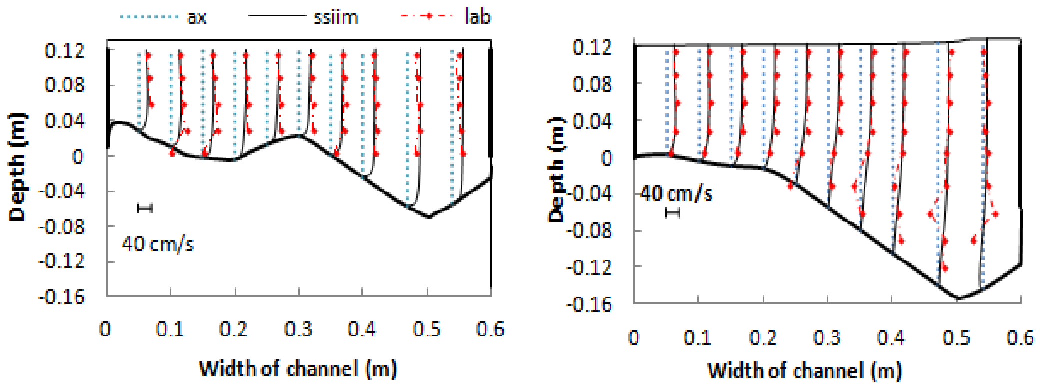

(a) (b)

Figure 3: Longitudinal velocity in cross-section at a distance of (a) 2.9L to downstream (b) 0.7L to upstream

3.0 Results and Discussion

3.1 Flow Pattern in Plan

Figures 4-5 show the flow patterns within the spur dike field at 10% of depth (at near the bed) and on water surface. From the figures, it is clear that in depth of near the bed, a part of flow moves toward inner bank but on water surface, the flow moves toward outer bank because the centrifugal force overcomes to the other forces. It is observed that the spur dike diverts the mainstream from outer bank, therefore the banks stability increases and are prevented from erosion due to formation of vortices around the spur dikes. At all distances between spur dikes, near the water surface the mainstream passes parallel to the dike wing and by increasing the distances between spur dikes, it reaches to the outer bank at farthest distance. By increasing the distances between spur dikes, the sizes of vortexes become larger. The flow velocity is slow in layers near the bed therefore a part of flow enters into two spur dikes field and is converted to upward flow in upstream of the second spur dike (due to the approaching second spur dike); that is effective in the formation of the vortex at higher level of depth. When two spur dikes placed at 2.5 and 3.5 times of spur dike length from each other, the vortex of two spur dikes field is incomplete. Because near the outer bank, the streamlines move generally from the upstream of the second spur dike toward out of dikes field and join to the mainstream but in case that S=5L, a vortex is formed completely due to increasing the distance between the spur dikes. Finally at depth of near the bed and on water surface level, three vortexes are formed at upstream of the first spur dike, at range between two spur dikes and at downstream of the second spur dike which respectively are effective in the formation of the separation zone, the dikes field and the reattachment zone.

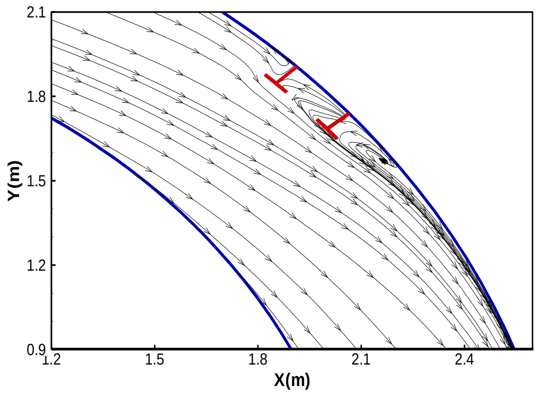

(a)

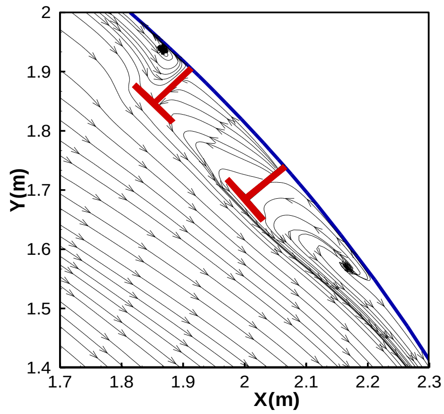

(a) zoom

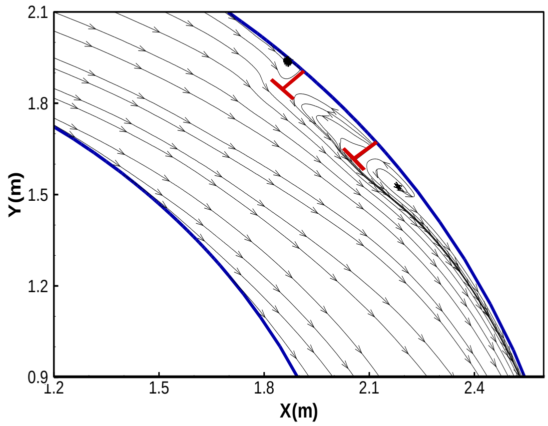

(b)

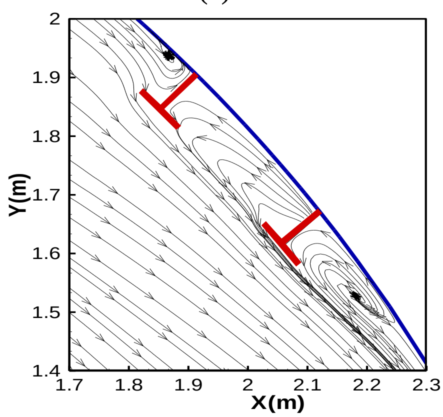

(b) zoom

Figure 4: Flow patterns on water surface when (a) S=2.5L (b) S= 3.5L (c) S=5L

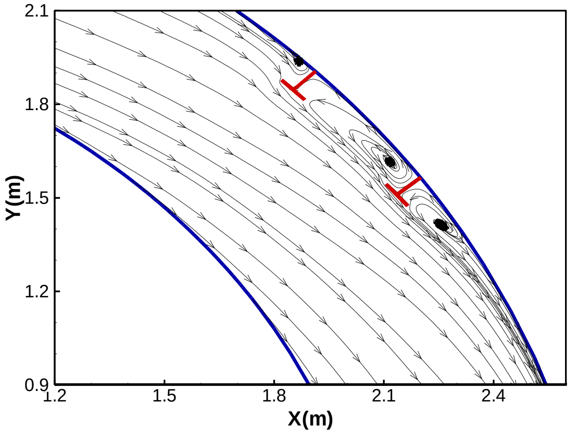

(c)

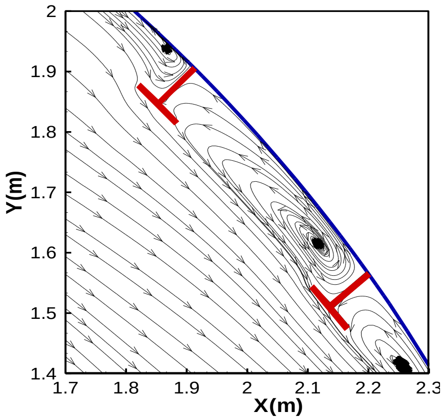

(c) zoom

Figure 4 (cont'): Flow patterns on water surface when (a) *S=2.5L* (b) *S= 3.5L* (c) *S=5L*

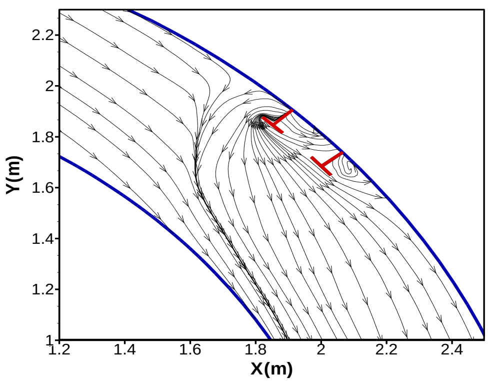

(a)

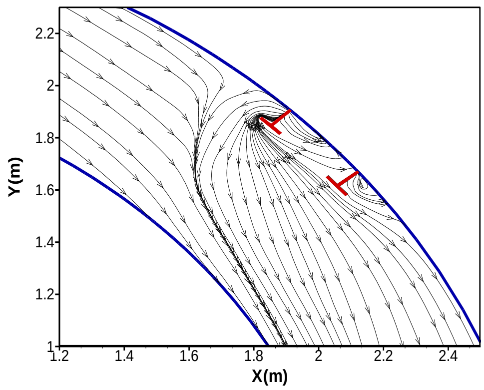

(b)

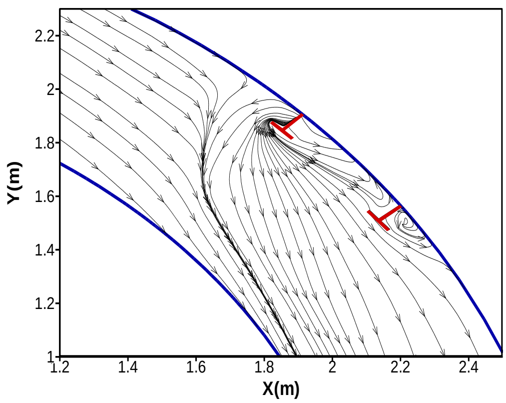

(c)

Figure 5: Flow pattern in level of 10% of flow depth from the bed when (a) *S=2.5L* (b) *S= 3.5L* (c) *S=5L*

3.2 Flow Pattern at Cross Section

As Figure 6(a), when S=2.5L a downward flow at downstream of the first spur dike can be seen due to formation of the vortex between spur dikes field, because in spur dikes field the flow moves from upstream of the second spur dike toward the first spur dike. In Figure 6(b) the central vortex between the first and the second spur dike in the mainstream path and a second vortex near the outer bank are observed; because the downward flow between two spur dikes is divided into two parts: One part moves toward the inner bank due to the influence of the secondary flow and leads to the formation of central vortex. Another part moves to outer bank and leads to the formation of vortex at outer bank. Figure 6(c) shows a cross section at downstream of the second dike wing, it is observed that downward flow is formed at downstream of dike wing as downstream of dike web.

Figure 6(d) shows the cross section at downstream of the second spur dike at a distance of 13.6L from the first spur dike which is comprised of two vortexes: a vortex in the center of channel and the larger vortex that it is inclined to the outer bank, because the mainstream and also the maximum longitudinal velocity are amenable to outer bank. These sections (the cross sections that were discussed above) were evaluated for other cases (S=3.5L and S=5L), the same cross sections were compared together that the comparative results are as follows: As Figure 7, the flow pattern is observed in case that S=3.5L. Figure 7(a) shows the cross-section at upstream of the second spur dike (that passes from the dike wing); three vortexes are formed on it: a central vortex due to the secondary flow, a vortex near the bed in front of the dike wing due to the interconnectedness between relatively weak upward flow from the bed and the stronger downward flow from the upper levels, and a vortex at the outer bank (third vortex).

The third vortex occurs near the water surface at outer bank, because the weak currents near the bed enter to dikes field and when they approach to the second spur dike are converted inevitably to upward flow due to the flow continuity and the pressure of upstream flow; then under the influence of centrifugal force, it moves toward inner edge of the second dike wing, therefore a small vortex is formed (the inner edge of dike wing showed in Figure 1(a)). Figure 7(b) shows the main and smaller vortexes at cross section in dike downstream, we can see that the smaller vortex is closer to the inner bank compared to when S= 2.5L. This vortex is formed due to the sedimentary bars near the inner bank. On the other hand, accumulation of sediments in the middle part of channel (that is caused by the main vortex), have created a sinking in the bed and thereupon this vortex (inner bank vortex) is formed. Figure 8 shows the flow pattern at two dikes field when S=5L. Parts of flow enter to the dikes field from the bed (because of the flow velocity is low) then converted to upward flow which is contrary to the streamlines of central vortex, as a result a small vortex is created near the outer bank.

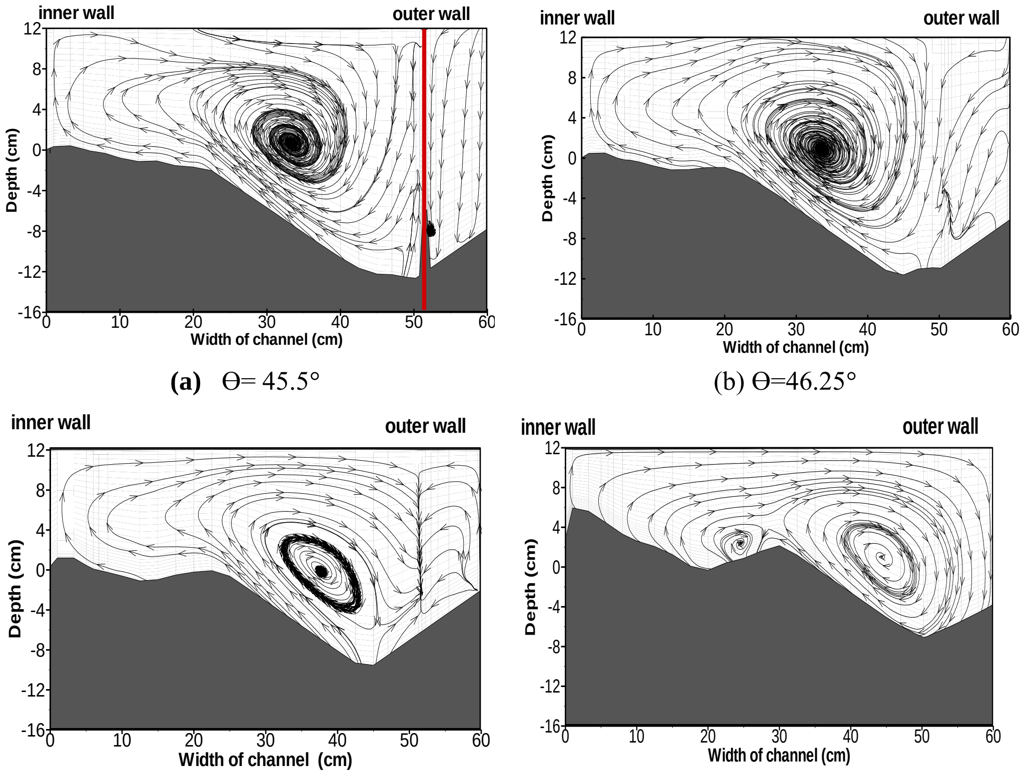

(a) ϴ= 45.5° (b) ϴ=46.25°

(c) ϴ=51° **(d)** ϴ=71°

Figure 6**:** Flow patterns when *S*=2.5*L* in cross section with distance of (a) 0.2*L* (b) 0.6*L* (c) 3*L* (d) 13.6*L* from the spur dike to downstream

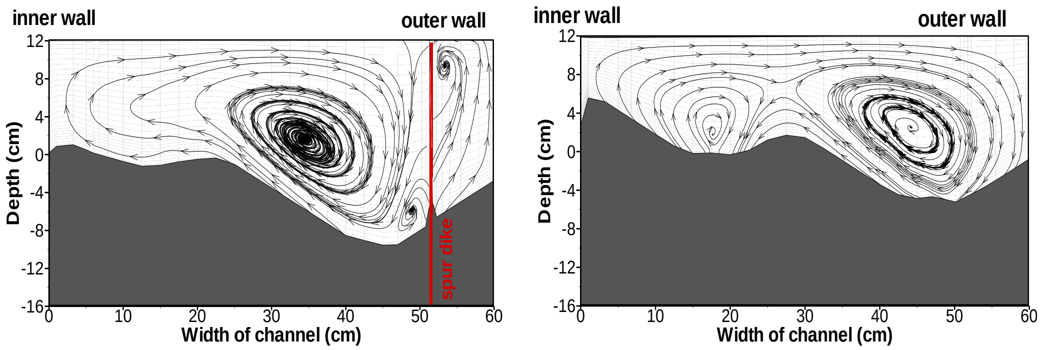

(a) ϴ=51° (b) ϴ=71°

Figure 7: Flow patterns when *S*=3.5*L* in cross section with distance of (a) 3*L* (b) 13.6*L* from the spur dike to downstream

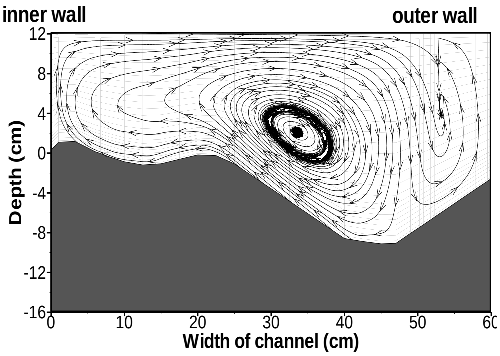

Figure 8: Flow pattern when S=5L in cross section with distance of 3L from the spur dike to downstream

4.0 Conclusions

By changing the position of two T-shaped spur dikes at 90° of bend, the flow patterns were compared at different section of bend. Following results are obtained:

1- By increasing the distances between spur dikes, the sizes of vortexes becomes larger. The flow velocity is slow in layers near the bed therefore a part of flow enters into two spur dikes field and be converted to upward flow in upstream of the second spur dike that is effective in the formation of the vortex at higher level of depth.
2- When *S=2.5L* and *S=3.5L*, the vortex of two spur dikes field is incomplete but in case that *S=5L,* a vortex is formed completely.
3- Near bed depth and on water level, three vortexes are formed at upstream of the first spur dike, at the range between two spur dikes and at the downstream of the second one which respectively are effective in the formation of the separation zone, field of two spur dikes and the reattachment zone.
4- It is observed that the size and number of vortex changes, this change is more obvious at location of spur dike and at spur dikes field.
5- At upstream of the second spur dike, three vortexes are formed: a central vortex, a vortex near the bed in front of the dike wing and a vortex at outer bank.
6- By increasing the distances between spur dikes, the mainstream reaches to the outer bank at farthest distance.
7- The downward flow between two spur dikes is divided into two parts: One part moves toward inner bank and leads to the formation of central vortex. Another part moves to outer bank and leads to the formation of vortex at outer bank.

References

Copeland, R.R. (1983). *Bank protection techniques using spur dikes*. Hydraulics Laboratory U. S. Army Engineer Waterways Experiment Station p. o. Box 631, Vicksburg, Miss. 39180.

Elawady, E., Michiue, M. and Hinokidani, O. (2001). *Movable bed scour around submerged spur-dikes*. Annual Journal of Hydraulic Engineering, JSCE, 45: 373-378.

Ghodsian, M. and Vaghefi, M. (2009). *Experimental study on scour and flow field in a scour hole around a T-shaped spur dike in a 90° bend*, International Journal of Sediment Research, 24: 145-158.

Mansoori, A.R., Nakagawa, H., Kawaike, K., Zhang, H., and Safarzade, A. (2012). *Study of the characteristics of the flow around a sequence of non-typically shaped spur dikes installed in a fluvial channel*, Annuals of Disas. Prev. Res. Inst., Kyoto Univ., No. 55B.

Mousavi, A.S., Mehrnahad, A.R., and Pirestani, M.R. (2012) *3-dimensional numerical model and laboratory for flow and bed deformation around a T-shaped spur dike in a 90° bend*, ICSE6 Paris, August 27-31.

Mousavi Naiini, S.A., Vaghefi, M., and Ghodsian, M. (2010). *Experimental investigation of rigid bed 90 degree bend relative radius's effects on changing of vorticity value around a T-shaped spure dike*, 8th International River Engineering Conference, Shahid Chamran University, 26-28 Jan., Ahwaz, Iran.

Muto, Y., Yasuyuki, B., and Shiro, A. (2002). *Velocity measurements in open channel flow with rectangular embayment formed by spur dikes*, Annuals of Disas. Prev. Res. Inst., Kyoto Univ., 45B-2: 449-457.

Naji Abhari, M., Ghodsian, M., Vaghefi, M., and Panahpur, N. (2010). *Experimental and numerical simulation of flow in a 90 degree of bend*, Flow Measurement and Instrumentation, 21: 292-298.

Olsen, N.R.B. (1999). *Computational fluid dynamics in hydraulic and sedimentation engineering*. Department of Hydraulic and environmental Engineering, Norwegian University of Science and Technology, Class notes, 2 nd. Revision.

Olsen, N.R.B. (2000). *CFD Algorithms for hydraulic Engineering*. Department of Hydraulic and environmental Engineering, Norwegian University of Science and Technology, Preliminary, 18. December, ISBN 82-7598-044-5.

Olsen, N.R.B. (2001). C*FD modeling for hydraulic structures*. Department of Hydraulic and environmental Engineering, Norwegian University of Science and Technology, Preliminary 1st edition, 8. May, ISBN 82-7598-048-8.

Olsen, N.R.B. (2009). *A three-dimensional numerical model for simulation of sediment movement in water intakes with multi-block option*. Department of Hydraulic and environmental Engineering, Norwegian University of Science and Technology, User's manual.

Schlichting, H. (1979). *Boundary-layer theory*. New York: McGraw-Hill. Seventh edition.

Shukry, A. (1950) Flow around bends in an open flume, Trans ASCE, American Society of Civil Engineers, 115(1): 751-779.

Sukhodolov, A., Engelhardt, C., Kruger, A., and Bungartz (2004) *Turbulent flow and sediment distribution in a groyne field*, Journal of Hydraulic Engineering, ASCE, 130(1): 1-9.

Suzuki, K., Michiue, M. and Hinokidani, O. (1987). *Local bed form around a series of spur dikes in alluvial channel*, Proceedings of the 22nd Congress of IAHR, Lausanne, Switzerland, August-September.

Vaghefi, M., Ghodsian, M., and Salehi Neyshabouri, S.A.A. (2012). *Experimental study on scour around a T-shaped spur dike in a channel bend*, Journal of Hydraulic Engineering, 138 (5): 471- 474.

Vaghefi, M., Shakerdargah, M., and Akbari, M. (2014). *Numerical study on the effect of ratio among various of submersion on 3-dimensional velocity components around T-shaped spur dike located in a 90 degree bend*, International Journal of Scientific Engineering and Technology, 3 (5): 675-679.

Vaghefi, M., Safarpoor, Y., and Hashemi, S.Sh. (2014). *Effect of T-shaped spur dike submergence ratio on the water surface profile in 90 degree channel bend using SSIIM numerical model*, International Journal of Advanced Engineering Applications, 7 (4):1-6.

Vaghefi, M., Safarpoor, Y., and Hashemi, S.Sh. (2015). *Effects of relative curvature on the scour pattern in a 90° bend with a T-shaped spur dike using a numerical method*, International Journal of River Basin Management, DOI: 10.1080/15715124.2015.1049181.

Van Rijn L.c. (2007). *Unified view of sediment transport by currents and waves: suspended transport*, Journal of hydraulic engineering, ASCE, 133: 668-689, DOI: 10.1061/(ASCE)0733-9429 (2007)133:6(668).

Wildhagen, J. (2004). *Applied computational fluid dynamics with sediment transport in a sharply curved meandering channel*. Institute for Hydromechanics University of Karlsruhe (TH), Germany.

Yossef, M.M. (2002). *the effect of groynes on rivers*. Delft University of Technology Faculty of Civil Engineering and Geosciences section of Hydraulic Engineering, pp17-23.